JOURNAL OF NEUROPHYSIOLOGY
Vol. 66, No. 4, October 1991. *Printed in U.S.A.*

A Fast Transient Potassium Current in Thalamic Relay Neurons: Kinetics of Activation and Inactivation

J. R. HUGUENARD, D. A. COULTER, AND D. A. PRINCE
Department of Neurology and Neurological Sciences, Stanford University Medical Center, Stanford, California 94305

SUMMARY AND CONCLUSIONS

1. Whole-cell voltage-clamp techniques were used to record K^+ currents in relay neurons (RNs) that had been acutely isolated from rat thalamic ventrobasal complex and maintained at 23°C in vitro. Tetrodoxin (TTX; 0.5 μM) was used to block Na^+ currents, and reduced extracellular levels of Ca^{2+} (1 mM) were used to minimize contributions from Ca^{2+} current (I_{Ca}).

2. In RNs, depolarizing commands activate K^+ currents characterized by a substantial rapidly inactivating (time constant ~20 ms) component, the features of which correspond to those of the transient K^+ current (I_A) in other preparations, and by a smaller, more slowly activating K^+ current, "I_K". I_A was reversibly blocked by 4-aminopyridine (4-AP, 5 mM), and the reversal potential varied with $[K^+]_o$ as predicted by the Nernst equation.

3. I_A was relatively insensitive to blockade by tetraethylammonium [TEA; 50%-inhibitory concentration (IC_{50}) $\gg$ 20 mM]; however, two components of I_K were blocked with IC_{50}s of 30 μM and 3 mM. Because 20 mM TEA blocked 90% of the sustained current while reducing I_A by <10%, this concentration was routinely used in experiments in which I_A was isolated and characterized. To further minimize contamination by other conductances, 4-AP was added to TEA-containing solutions and the 4-AP–sensitive current was obtained by subtraction.

4. Voltage-dependent steady-state inactivation of peak I_A was described by a Boltzman function with a slope factor (k) of −6.5 and half-inactivation ($V_{½}$) occurring at −75 mV. Activation of I_A was characterized by a Boltzman curve with $V_{½}$ = −35 mV and k = 10.8.

5. I_A activation and inactivation kinetics were best fitted by the Hodgkin-Huxley m^4h formalism. The rate of activation was voltage dependent, with τ_m decreasing from 2.3 ms at −40 mV to 0.5 ms at +50 mV. Inactivation was relatively voltage independent and nonexponential. The rate of inactivation was described by two exponential decay processes with time constants (τ_{h1} and τ_{h2}) of 20 and 60 ms. Both components were steady-state inactivated with similar voltage dependence.

6. Temperature increases within the range of 23–35°C caused I_A activation and inactivation rates to become faster, with temperature coefficient (Q_{10}) values averaging 2.8. I_A amplitude also increased as a function of temperature, albeit with a somewhat lower Q_{10} of 1.6.

7. Several voltage-dependent properties of I_A closely resemble those of the transient inward Ca^{2+} current, I_T. This would, in turn, lead to concurrent activation of these two opposing conductances under physiological circumstances. Therefore, to directly compare I_A vis-à-vis I_T, we used pharmacological procedures in single cells to determine the voltage dependencies of activation and inactivation. Although I_A and I_T activate and inactivate with similar time courses, the steady-state inactivation and activation functions are 10–20 mV hyperpolarized for I_T compared with I_A. Implications of the interactions between I_A and I_T in relation to regulation of RN spike-firing modes are discussed.

INTRODUCTION

Recent biophysical studies using various voltage-clamp techniques (Coulter et al. 1989a; Crunelli et al. 1989; Hernández-Cruz and Pape 1989; Suzuki and Rogawski 1989) have demonstrated an important transient Ca current (I_T) in thalamic relay neurons (RNs) that is both necessary and sufficient for the generation of Ca-dependent, low-threshold spikes (LTS). The latter are deinactivated during membrane hyperpolarizations from rest and can trigger bursts of Na^+-dependent action potentials. Such bursting behavior becomes a prominent feature of RN activity during behavioral states associated with drowsiness (Steriade and Llinás 1988) and perhaps certain forms of epilepsy (Coulter et al. 1989b). The firing mode of RNs, i.e., single spikes versus burst firing, is a pivotal factor in determining whether peripheral sensory information will be faithfully transmitted to the cerebral cortex (Steriade and Llinás 1988). Thus both intrinsic and extrinsic factors that affect activation or inactivation of I_T have critical influences on thalamocortical excitation and behavior.

One such intrinsic property that would be expected to influence LTS generation is activation of voltage-gated K^+ conductances. K^+ current activation might slow or retard the development of Ca-dependent spikes and influence their repolarization. It has been hypothesized from the results of current-clamp recordings that RNs contain a sizable transient K^+ current, I_A, which can function to slow the approach of the membrane potential to firing threshold after a hyperpolarization (Jahnsen and Llinás 1984). However, hyperpolarization will also concurrently deinactivate the LTS and thus promote burst firing. Therefore the following question arises: in the presence of a considerable and opposing transient K^+ current, how is it possible for the transient Ca^{2+} current to generate a LTS? In this study we have exploited the ability to characterize multiple currents in single cells through the use of rapid extracellular perfusion of appropriate ion-channel blockers. This then allows direct comparison of voltage dependence of the I_A and I_T by eliminating systematic errors (such as variability in diffusional or liquid-junction potentials) that occur when these ionic currents are characterized in separate populations of cells. This is a further step toward the final goal of modeling

voltage behavior in RNs and increasing our understanding of regulation of firing pattern in the thalamus. Preliminary results have been published in abstract form (Huguenard et al. 1990).

METHODS

Cell preparation

RNs were acutely isolated from the ventrobasal (VB) complex of 7- to 15-day-old Sprague-Dawley rats as previously described (Coulter et al. 1989a), using a modification of the technique described by Kay and Wong (1986). Briefly, animals were anesthetized with pentobarbital sodium (50 mg/kg) and decapitated, and the brain was removed. Coronal sections were cut on a vibratome at a thickness of 500 μm. Slices containing VB were incubated for 45–90 min in oxygenated PIPES-buffered saline (see *Solutions*) containing trypsin (Type XI, 8 mg/10 ml), then rinsed in enzyme-free solution. Using appropriate landmarks (Coulter et al. 1989a), we subdissected chunks of VB (~1 × 2 mm), triturated them with Pasteur pipettes, and plated the cell suspensions onto 35-mm plastic petri dishes. Isolated neurons survived for up to 12 h at room temperature, as judged by their appearance under modulation contrast optics and by their capacity to generate a variety of voltage-dependent currents.

Solutions

PIPES-buffered saline consisted of (in mM) 120 NaCl, 5 KCl, 1 $MgCl_2$, 1 $CaCl_2$, 25 glucose, and 20 piperazine-*N,N'*-bis[2-ethanesulfonic acid] (PIPES); and the pH was adjusted to 7.0 with NaOH (Kay and Wong 1986). For whole-cell recording of K^+ currents the following intracellular solution was used (in mM): 130 KCl, 10 *N*-2-hydroxyethylpiperazine-*N'*-2-ethanesulfonic acid (HEPES), 11 ethyleneglycol-bis-(β-aminoethyl ether)-*N,N,N',N'*-tetraacetic acid (EGTA), 1 $MgCl_2$, 1 $CaCl_2$, and 4 Na_2 ATP, pH 7.3. An ATP regeneration system (creatinine phosphokinase 50 U/ml and phosphocreatine 22 mM; see Coulter et al. 1990; Forscher and Oxford 1985) was made fresh daily and added to the intracellular solution in all recordings because this was found to dramatically increase the quality and duration of whole-cell recordings. Osmolality of both intracellular and extracellular solutions was adjusted to 305 mosmol/kg H_2O before each experiment. The extracellular solution consisted of (in mM) 155 NaCl, 3 KCl, 1 $MgCl_2$, 1 $CaCl_2$, 0.0005 tetrodotoxin (TTX), and 10 HEPES, with pH adjusted to 7.4. With 1 mM extracellular Ca^{2+}, there was some contribution of Ca^{2+} current (I_{Ca}) to the total whole-cell current. This concentration of Ca^{2+} was chosen as a compromise that balanced reduced cell viability at low [Ca^{2+}] with interference from I_{Ca} at higher concentrations. Under these conditions maximum I_{Ca} was normally <200 pA, compared with maximum K^+ current of >5 nA, and thus I_{Ca} would contribute <5% of the total whole-cell current.

All chemicals were obtained from Sigma (St. Louis, MO). Dendrotoxin I was a kind gift of M. Lazdunski. When extracellular tetraethylammonium chloride (TEA-Cl) was used, it was substituted for equimolar NaCl. Solution changes were obtained by use of the "sewer pipe" technique (Yellen 1982), in which several solutions flow out of parallel Teflon tubes in a laminar pattern. Rapid (<100 ms) and complete solution changes at constant flow rate were then effected by moving the tube assembly in relation to the neuron under study.

Electrophysiological recordings

Isolated RNs were voltage-clamped using the whole-cell configuration of the patch-clamp (Hamill et al. 1981). Electrodes were pulled from medium-walled borosilicate glass (Garner Glass, Claremont, CA; KG-33, 1.8-mm OD, 1.3-mm ID) on a List L/M-3P-A (Medical Systems, Great Neck, NY) puller using a two-step procedure. Electrode resistances were 2–4 MΩ in the bath. A small liquid junction potential (<4 mV) was measured between the intracellular and extracellular solutions and was not compensated. Current recordings were obtained with the List EPC-7 amplifier (Medical Systems). Series resistance compensation was used to eliminate >90% of the voltage error due to voltage drop across the electrode. Access resistance was normally in the range of 4–10 MΩ. K^+ currents in RNs are often quite large, and so even with compensation, significant voltage errors can occur. The magnitude and consequences of the error in various experiments are indicated in RESULTS and in the figure legends. A modified P/X leak subtraction technique was used to eliminate leak and capacitative currents (Bezanilla and Armstrong 1977; Coulter et al. 1989a). In most cases, experiments were performed at room temperature (22–24°C) to prolong survival of isolated cells. In a few cases, the temperature in the chamber was increased to 24–35°C by warming the petri dish chamber with a feedback-controlled resistive heater. Temperature was monitored locally with a small thermocouple placed in the chamber within 0.2 mm of the cell under study.

Data storage and analysis

Data were acquired on-line in either unsubtracted or leak-subtracted form by use of a DEC 11/73-based computer equipped with the Cheshire interface (Indec Systems, Sunnyvale, CA) running under BASIC-23. For kinetic fits to current records, an iterative approach was used in which the parameters were adjusted by means of the analog inputs on the Cheshire interface. This method was found to provide a rapid means of fitting onsets and exponential decays with up to two components. A nonlinear least-squares fitting routine (simplex method; Caceci and Cacheris 1984) was used to obtain nonbiased estimates of parameters describing Boltzman functions and concentration response curves.

RESULTS

K^+ currents in RNs

Acutely isolated neurons were prepared for this study as described previously (Coulter et al. 1989a). The dissociation procedure resulted in somewhat truncated neurons with triangular or pear-shaped soma [typically 15 × 30 μm (minimal and maximal diam)] and between one and four dendrites (1.5- to 3-μm diam and 40- to 60-μm length). In a limited sample of cells, membrane capacitance, as measured by integrating the current response to a small voltage step, was 17.5 ± 0.63 (SE) pF (n = 38). As part of a study of K^+ currents in acutely isolated hippocampal neurons, Numann et al. (1987) have estimated steady-state voltage attenuation at the end of dendrites to be <10% during an active response. Isolated RNs [estimated electrotonic length (L) <0.1] have dendrites with diameters similar to but lengths shorter than their counterparts from the hippocampus, so 10% attenuation is a conservative estimate for the maximal error in the present study. Therefore space clamp considerations are not likely to be a complicating factor in the interpretation of voltage-clamp records obtained with dissociated RNs.

Under ionic conditions that isolate K^+ currents (see METHODS), depolarizing voltage-clamp commands evoke

outward currents, as illustrated by the traces in Fig. 1. The control traces in Fig. 1*A* illustrate that, with depolarizations in the range of −55 to −40 mV, a prominent transient outward current is evident that appears similar to I_A as described in several cell types (Rogawski 1985). Depolarizations to potentials more positive than −40 mV result in currents that are not fully inactivating, yet the transient component is still dominant. Figure 1*B* shows traces from the same cell obtained with the addition of 20 mM TEA to the extracellular solution. TEA blocks most of the delayed K^+ current with little effect on I_A (Thompson 1977), so that the resultant currents become nearly completely inactivating within 300 ms (Figs. 1, *B* and *C*, and 2). The current-voltage (*I-V*) relationships for early current (5 ms) and late current (300 ms) in Fig. 1*C* show that the early current, which was mostly due to I_A, was activated at more negative potentials than the late current and attained a higher amplitude. Figure 1*C* also shows that TEA selectively blocked the late current with little effect on the early current. The smooth curves in Fig. 1*C* are fitted Boltzman activation functions of the form

$$g = \frac{g_{max}}{1 + \exp\left[\frac{V - V_{½})}{k}\right]} \quad (1)$$

where $V_{½}$ is the voltage at which the conductance is one-half activated, V is the membrane command potential, k is the slope factor, g_{max} is the maximum conductance, and I is given as

$$I = g(V - V_K) \quad (2)$$

where V_K is the reversal potential for K^+. Normalized conductance curves in Fig. 1*D* emphasize the differences in voltage-dependent activation of these two currents. The fitted curves (*Eq. 1*) do not represent the data adequately, probably owing to concurrent activation of multiple conductances. Nevertheless, the fitted values provide a means of characterizing "early" vs. "late" K^+ currents to demonstrate the dominance of early, inactivating component. Group data for VB neurons are given in Table 1, which shows that early currents activate at more negative membrane potentials and are associated with a maximum conductance >2 times higher than the late currents. Because the composite K^+ currents are difficult to identify under these conditions, we used a variety of voltage-clamp protocols and pharmacological agents to isolate and analyze the transient K^+ current.

TEA sensitivity of RN K^+ currents

Our first approach was to expose neurons to TEA to block delayed K^+ currents. Because little was known about

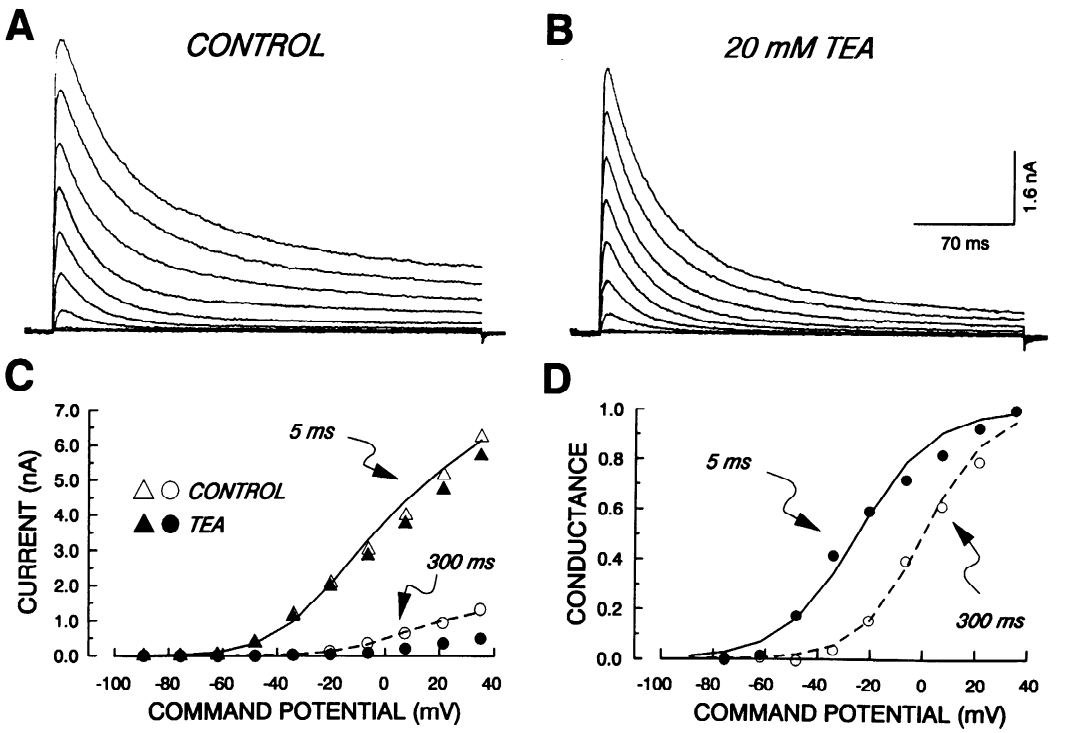

FIG. 1. TEA sensitivity of transient and persistent outward currents in relay neurons. *A* and *B*: voltage-clamp steps (300-ms duration with +14-mV increments between −90 and +36 mV) were applied from a holding potential of −100 mV in control solution (*A*) and with perfusate containing 20 mM TEA (*B*). A rapidly activating and inactivating current component is observed at potentials positive to −60 mV and is insensitive to TEA. Amplitude of this early peak current is shown in *C* (△). Persistent current, at 300-ms latency, is smaller in amplitude (○), has a higher threshold, and is reduced by TEA. *C*: *I-V* relationships for the 2 situations in *A* and *B*. Smooth curves are attempts to fit Boltzman activation functions to the currents. *D*: activation curves normalized to maximal conductance for each component. Current at 5-ms latency has a much lower threshold than the persistent current. Note the inadequacy of the fitted curves, especially for the current at 5-ms latency. Fitting parameters were as follows: at 5-ms latency, g_{max} = 49.4 nS, $V_{½}$ = −25 mV, and k = 14; at 300 ms latency, g_{max} = 10.5 nS, $V_{½}$ = 0 mV, and k = 12; E_K was assumed to be −87 mV for each latency (see Fig. 5). Maximum R_s error 12 mV.

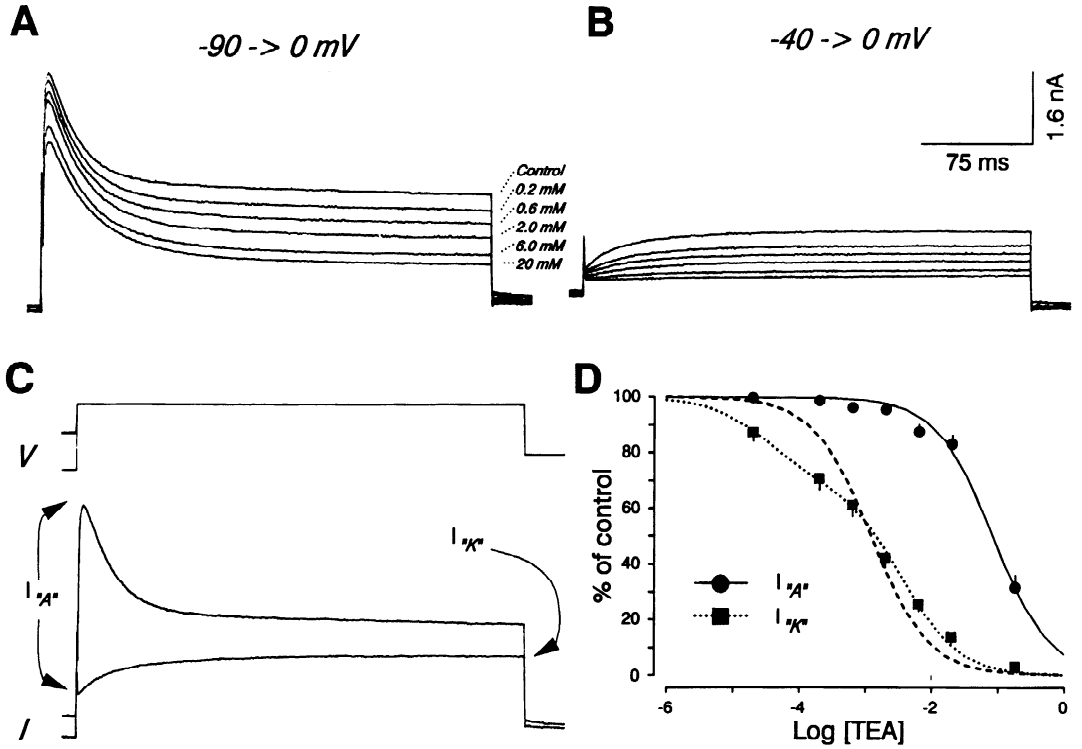

FIG. 2. TEA sensitivity of I_K. *A*: repeated voltage-clamp commands to 0 mV were elicited at 0.1 Hz while holding potential was alternated between −90 and −40 mV. Effects of TEA were immediate on solution change, and ≥3 successive current responses were obtained and averaged at each concentration. Increasing concentrations of TEA decreased the current level throughout the duration of the pulse. Even at the highest TEA concentration, a large transient current is evident. *B*: currents obtained from V_{hold} of −40 mV. No transient current is seen, and increasing concentrations of TEA (in the same range as in *A*) incrementally block the persistent current. *C*: method of measuring I_A and I_K for the TEA concentration response curve in *D*. I_A was measured as the difference in short-latency (5 ms) currents when the holding potential was changed from −90 to −40 mV. I_K was the persistent current at the end of the 300-ms depolarization from V_{hold} −40 V. *D*: concentration response curves for I_A and I_K in relay neurons. I_A was relatively insensitive to TEA. Fitted curve (——) is calculated for a single binding site with an affinity of 83 mM. In contrast, I_K was very sensitive to TEA, but the results could not be well fitted by assuming interactions with 1 binding site (dashed line is best fitted single Langmuir isotherm: K_D = 2.3 mM). Dotted line is the composite blocking effect expected with 2 binding sites with K_Ds of 33 μM and 3.6 mM, with the higher affinity site contributing 31% to the total block. Error bars represent SE; *n* is ≥5 cells for each concentration. Maximum R_s error 2.5 mV.

the concentration dependence of this action of TEA on RNs, experiments were performed to evaluate the blocking action of this agent on non-I_A-type currents. Results from a typical concentration-response experiment are shown in Fig. 2, *A* and *B*. Bath solutions containing 0.2–20 mM TEA produced concentration-dependent blockade of the delayed current. The early transient current, I_A, obtained with a V_{hold} of −90 mV was much less affected by TEA (Fig. 2*A*) than the delayed current. When the holding potential was set to −40 mV, no rapidly inactivating component could be evoked; i.e., I_A was completely inactivated. Under these conditions, the late current amplitude was reduced compared with that obtained with a more hyperpolarized V_{hold} (cf. delayed currents in Fig. 2*C*), indicating that I_K undergoes significant steady-state inactivation in these cells.

TABLE 1. *Activation properties of early and late outward currents in relay neurons*

	$V_{1/2}$, mV	k	g_{max}, nS	n
Early (5 ms)	−25.6 ± 2.0	14.3 ± 0.8	55.2 ± 9.4	11
Late (300 ms)	−5.3 ± 1.3	13.0 ± 0.4	20.7 ± 4.8	11

Values are means ± SE; *n*, number of cells. $V_{1/2}$, voltage at which the conductance is one-half activated; *k*, slope factor; g_{max}, maximum conductance.

The concentration-response curves for "I_A" and "I_K" (quotes to indicate that these do not represent completely isolated currents) as measured in Fig. 2*C* are shown in Fig. 2*D*. I_A is relatively insensitive to TEA, whereas I_K is comprised of two separate components with 50%-inhibitory concentrations (IC_{50}s) of ~33 μM (31% of total TEA-sensitive current) and 3.6 mM (69% of total). A similar biphasic concentration-response curve was obtained for the effect of TEA on the late current when V_{hold} was hyperpolarized to −90 mV (not shown). In this case the best-fitted curve again provided evidence for two blockade sites: a high-affinity site (IC_{50} = 25 μM, 16% of total) and a low-affinity site (4.1 mM, 84% of total). The current blocked by the low-affinity (mM) site must then account for most of the steady-state inactivation of the delayed current, because its contribution to total current is reduced when the holding potential is made less negative. A complete description of the kinetic properties of late I_K components is reported elsewhere (Hu-

guenard and Prince 1991). However, it is important to note here that 20 mM TEA blocked ~90% of the delayed current but only 10–15% of I_A (Fig. 2*D*). This concentration was used in further experiments as a selective blocker of the delayed current.

Steady-state inactivation of I_A

One of the most prominent and consistent features of I_A in a variety of cell types and preparations is that of steady-state inactivation (reviewed by Rogawski 1985). In many types of cells, I_A is inactivated at normal resting potentials and requires prior hyperpolarization before activation can occur. I_T in thalamic neurons is also characterized by this property (Coulter et al. 1989a; Crunelli et al. 1989; Hernández-Cruz and Pape 1989; Suzuki and Rogawski 1989). There are many other similarities between these two currents in terms of both their voltage dependencies and time courses (e.g., Fig. 3, *A* vs. *B*). Under physiological conditions, the net membrane potential deflections resulting from activation of both I_A and I_T will depend on several variables, including the steady-state availability of each current.

Because these two currents are expected to interact during LTS generation, we examined steady-state inactivation properties of I_A and compared them with those of I_T in experiments in which it was possible to isolate and measure both currents in the same neuron. This approach allowed stringent comparison of voltage dependencies of I_A and I_T, because it minimized or eliminated junction potential and other procedural differences obtained when recording from separate neurons with different intracellular solutions. Standard steady-state inactivation protocols were used in which the prepulse potential was varied before activation steps to −40 mV. This command potential activated mainly I_A and I_T because it was outside of the activation range for delayed I_K. Somewhat surprisingly, "I_A" amplitude showed biphasic voltage dependence. With the most hyperpolarized values of V_{hold} (*traces 1* and *2*, the peak amplitudes of which are marked with arrow in Fig. 3*A*), the transient outward current was not maximal and became larger, then smaller, as V_{hold} was made gradually less negative (see I_{total} in Fig. 3*D*). When the K^+-channel blockers 4-AP (5 mM) and TEA (20 mM) (Thompson 1977) were added to the extracellular solution, the transient outward current was

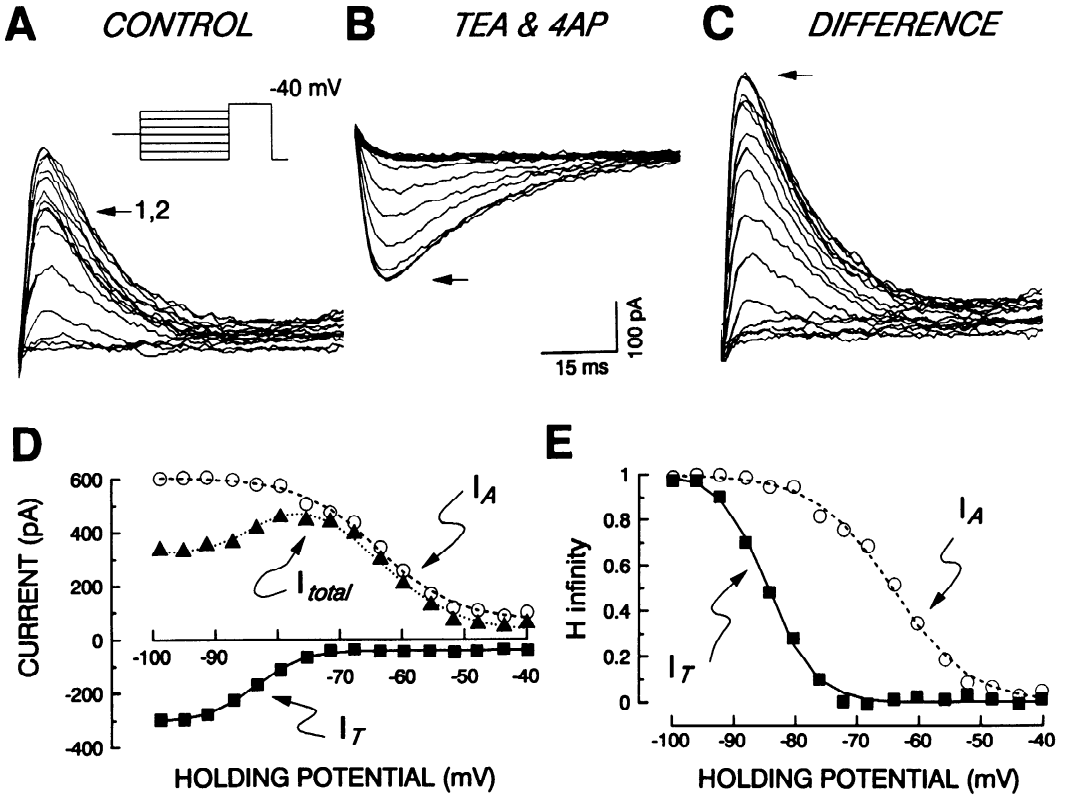

FIG. 3. Overlapping voltage dependence of steady-state inactivation for T current and A current in the same neuron. *A*: depolarizing commands to −40 mV were preceded by 1-s conditioning steps to various potentials, as illustrated in the voltage protocol shown in the *inset*. Currents evoked with the most hyperpolarizing conditioning pulses are indicated by the arrow in parts *A–C*. *B*: with 20 mM TEA and 5 mM 4-AP included in the bath solution, the same voltage protocol now produced inward currents (T currents), which monotonically decreased with increasingly depolarized conditioning potentials. *C*: current traces from *B* are subtracted from those in *A* to obtain the 4-AP/TEA-sensitive currents. As in the case of the isolated T current in *B*, the A current isolated by this procedure demonstrates monotonic steady-state inactivation. *D*: steady-state inactivation curves for the 3 situations in *A–C*, with fitted Boltzman functions. I_{total} refers to the control situation in *A*, I_T to the currents in *B* (fitted curve parameters: $V_{½} = -83$ mV, $I_{max} = 263$ pA, and $k = 3.8$), and I_A to *C* (parameters: $V_{½} = -63$ mV, $I_{max} = 535$ pA, and $k = 6.2$). *E*: normalized h_∞ curves from data in *D*. $[Ca^{2+}]_o$ was increased to 3 mM in this experiment to increase the amplitude of the T current and allow comparison of the inactivation properties of I_A and I_T in the same cell. Maximum R_s error <1 mV.

TABLE 2. *Steady-state inactivation and voltage-dependent activation of 4-AP-sensitive current in relay neurons*

	$V_{1/2}$, mV	k	n
Activation	−36.1 ± 2.2	10.8 ± 0.6	10
Inactivation	−74.7 ± 1.0	6.3 ± 0.1	18

Sigmoid curves were fitted to raw data by means of a nonlinear least-squares routine. Values are means ± SE; n, number of cells. Abbreviations, see Table 1.

blocked and a transient inward current I_T was uncovered (Fig. 3*B*). I_A, obtained as the 4-AP-sensitive current by subtraction, exhibited monotonic steady-state inactivation (Fig. 3, *C* and *D*). The steady-state inactivation functions for I_T (in the presence of 4-AP/TEA) and I_A (4-AP-sensitive current) could thus be determined in the same cell. In the example of Fig. 3, *D* and *E*, it is clear that I_A required less hyperpolarization to remove inactivation than I_T and could therefore be activated from voltages nearer to resting membrane potential (cf. data of Table 2 on steady-state inactivation of I_A with those for I_T in Coulter et al. 1989a).

For demonstration purposes, $[Ca^{2+}]_o$ was increased to 3 mM in the experiment shown in Fig. 3. In other experiments, steady-state inactivation of I_T (in 4-AP/TEA) and I_A (4-AP-sensitive current in TEA) was determined in such fashion for six cells in the presence of 1 mM $[Ca^{2+}]_o$. In some cases the sequence of solution changes was reversed to eliminate any possible systematic errors in the pharmacological subtraction produced by voltage drift or rundown of currents. Results similar to those in Fig. 3 were seen in all cases. In terms of LTS generation, the significance of this interaction is that, when I_T is activatable, I_A is also available for activation and can either slow the rising phase of the LTS to delay its onset or block it completely. This effect will be considered further in the DISCUSSION.

Activation of I_A and relationship to I_T

The voltage dependence of I_A activation was measured (n = 10) by the use of a 4-AP-subtraction procedure as

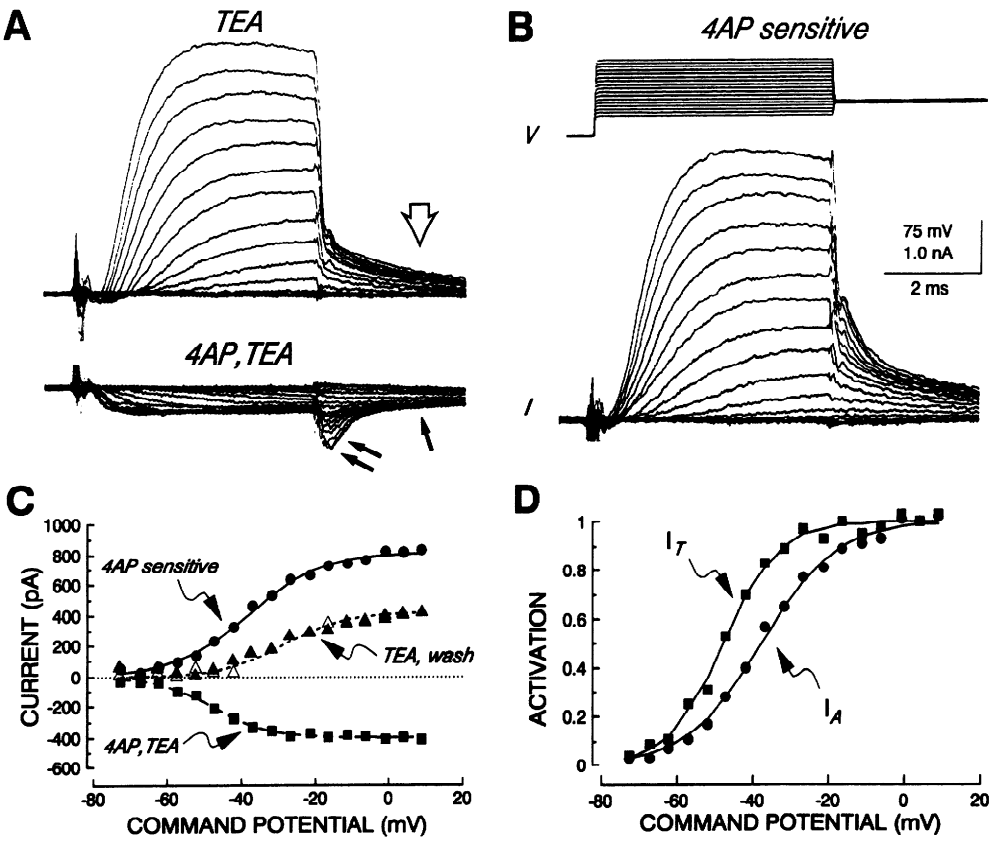

FIG. 4. Activation of I_A and I_T compared in the same cell. *A, top traces*: leak-subtracted currents obtained with 4-ms depolarizations from a holding potential of −100 mV. In 20 mM TEA and with short-duration pulses, an outward current (I_A) is relatively isolated from other K currents, but not from I_T. Tail current amplitude (at 2.4-ms latency, see ⇩) at a potential of −50 mV was used as a measure of activation. With addition of 5 mM 4-AP to the extracellular solution, the same protocol now produces only inward currents (*bottom traces*). Inward tail currents are composed of 2 parts: a slowly decaying component (↖, T-current deactivation) attains peak amplitude with voltage commands positive to −20 mV, and a rapidly inactivating component (↖↖, L current) is seen with depolarizing commands positive to −30 mV. T-current amplitude was measured in isolation (2.4-ms latency) and is given in *C* as the filled squares. *B*: activation of I_A. *Top traces*: voltage protocol (*V*) for *A* and *B*. *Bottom traces* (*I*): are 4-AP-sensitive currents, obtained by subtracting *bottom traces* from *top traces* in *A*. Activation has a threshold near −60 mV and saturates near 0 mV. *C*: activation curves for currents in *A* and *B*, as well as the wash currents obtained on returning to 4-AP-free solution. Filled triangles, TEA; filled squares, 4-AP and TEA; filled circles, 4-AP blocked; and open triangles, wash. *D*: activation curves for 4-AP-sensitive current (I_A) and inward current in presence of TEA and 4-AP (I_T) are normalized to maximum current. Fitted curve parameters are, for I_T, $V_{½}$ = −48 mV, I_{max} = −398 pA, and k = 7.4; and for I_A, $V_{½}$ = −38.1 mV, I_{max} = 820 pA, and k = 9.8. Maximum R_s error = 2.5 mV.

above. Brief depolarizing commands (4 ms) were applied in either TEA (to elicit I_T and I_A; Fig. 4*A*, *top*) or in 4-AP–TEA (to elicit I_T alone; Fig. 4*A*, *bottom*). Tail current amplitude was used as an index of activation for both I_T and I_A, because it was always measured at the same potential and was thus normalized for driving force. Activation curves for I_A and I_T are shown in Fig. 4, *C* and *D*, where it can be seen that the two currents have similar activation thresholds, but that the steepness of activation is greater for I_T, so that the voltage at which the current is half-maximally activated is ~10 mV more depolarized for I_A than for I_T. The steeper and less depolarized activation of I_T relative to I_A may contribute to the regenerative depolarization that is characteristic of the LTS. Averaged data for activation of I_A are given in Table 2. Maximum tail current amplitude as measured by the tail current protocol was 750 ± 40 (SE) pA. With a K^+ equilibrium potential (E_K) of −87 mV (and assuming I_A tails had decayed by ½ at the time of measurement; see Fig. 4*B*), this results in a calculated maximum conductance of 40 nS. Because the average capacitance of isolated RNs was 17.5 pF, the normalized conductance would be 2.3 nS/pF or 23 pS/μm^2, assuming a membrane capacitance of 1 μF/cm^2. In the same group of cells, maximum I_T tail current amplitude was 360 ± 16 pA. If it is assumed that Ca^{2+} equilibrium potential (E_{Ca}) is +30 mV (Coulter et al. 1989a), normalized conductance for I_T would be 4.5 nS (0.26 nS/pF or 2.6 pS/μm^2). Evidence that tail currents recorded in the presence of TEA–4-AP actually represent I_T is provided by the finding that essentially the same activation curve is seen under separate and distinct recording conditions that isolate I_{Ca}: intracellular solutions containing tris(hydroxymethyl)aminomethane (Tris)-PO_4 (Coulter et al. 1989a) and TEA-Cl/$CaCl_2$ (0 Na^+, 0 K^+) in the extracellular perfusate (n = 10, data not shown).

K^+ dependence of I_A

The reversal potentials of tail currents were used as a measure of the equilibrium potential of the transient K^+ current (E_A), which was found to vary linearly with the logarithm of $[K^+]_o$ (Fig. 5). Tail current amplitude was measured in leak-subtracted traces at a latency of 0.5 ms from the termination of the command step (Fig. 5, *A* and *B*). Elevating $[K^+]$ from 3 to 30 mM resulted in a depolarizing shift in the reversal potential from −87 to −35 mV (Fig. 5*C*). The results from group data are given in Fig. 5*D*, with the solid line indicating the predicted E_K based on a calculated intracellular K^+ activity of 110 mM. A small deviation from the Nernst potential is seen with 3 mM K; it may be due to two factors: $[K^+]_o$ accumulation during the com-

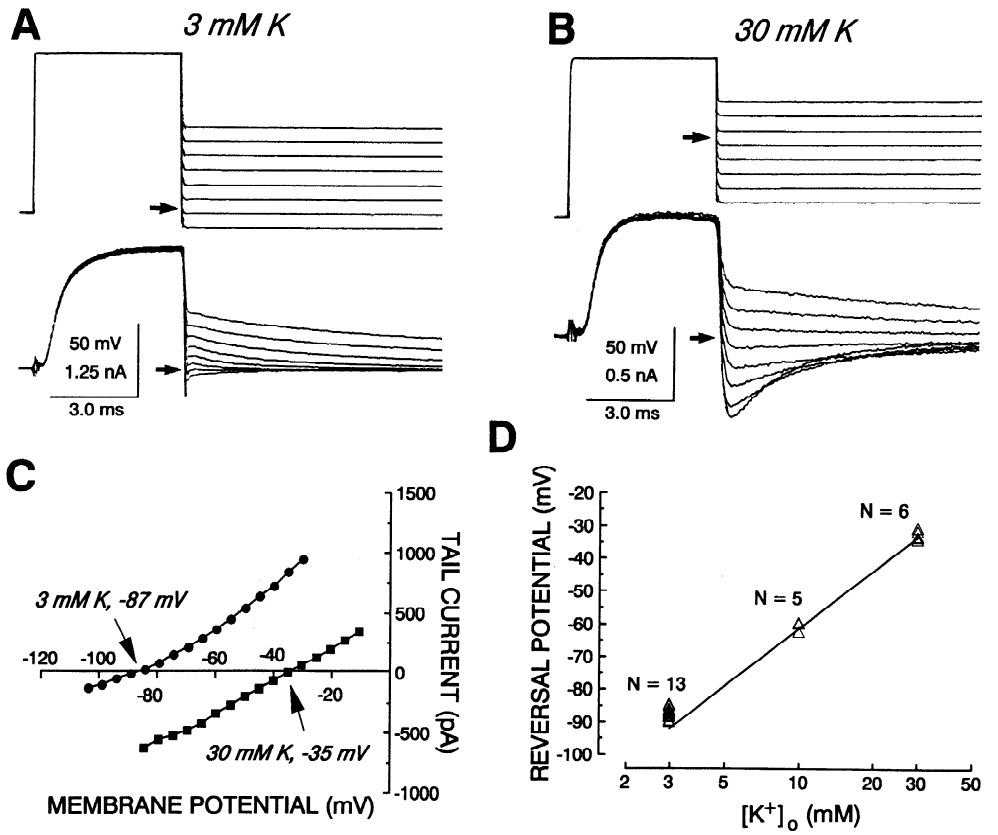

FIG. 5. K^+ dependence of I_A in relay neurons. *A*: brief (5 ms) depolarizations to +20 mV were used to activate I_A. Membrane potential was then repolarized to various levels and tail current amplitude and polarity were measured. With 3 mM $[K^+]_o$, reversal was between −80 and −90 mV [see → on voltage (*top*) and current (*bottom*) traces]. *B*: changing $[K^+]_o$ to 30 mM in the same cell caused a shift in reversal to between −30 and −40 mV. Note the faster rate of tail current decay at the most hyperpolarized potentials. *C*: reversal potential plots for the 2 situations in *A* and *B*. Current traces shown in *A* and *B* are a subset of total currents measured in *C*. *D*: group data for dependence of E_A on $[K^+]_o$. At each K^+ concentration, each symbol is a different cell. Solid line is the calculated reversal potential for a Nernst function with intracellular K^+ activity of 110 mM at 23°C. Maximum R_s error 2.5 mV.

mand pulse (Frankenhaeuser and Hodgkin 1956) or contribution of other ions (including Na^+) to I_A permeability. The latter explanation is more likely, because there should be little opportunity for accumulation in locally superfused isolated neurons, except perhaps in the area of contact between the cell and the tissue culture dish. In fact, the deviation from Nernst potential can be explained by a permeability ratio of 0.004 (pNa:pK).

Voltage dependence of kinetic rate constants for I_A

To study the kinetics of I_A activation and inactivation, we again used pharmacological subtraction. 4-AP is thought to be a relatively selective blocker of I_A (Thompson 1977); however, we found that it blocked delayed currents as well. For example, at 5 mM it blocked ~30% of the delayed current measured at 300-ms latency. Therefore we first blocked delayed currents with 20 mM TEA before the addition of 4-AP. Under these conditions, the IC_{50} for I_A blockade with 4-AP was ~2 mM (data not shown). As in mollusc (Thompson 1977), the concentration-response curve was steeper than would be expected with a single, noncooperative binding site, and 5 mM 4-AP caused nearly complete blockade of I_A. In contrast to TEA, the effects of which were immediate on changing solutions, it took ~100 s for the 4-AP effect to reach equilibrium or to wash. With low concentrations (<1 mM) and during the period when the effects of higher concentration were coming to equilibrium, I_A inactivation was slowed and the late (300 ms) current was increased, consistent with voltage-dependent unblocking of 4-AP effects (Thompson 1982). This effect would invalidate the use of the pharmacological subtraction method described here, because I_A channels would be blocked to different extents throughout the depolarizing command, and the 4-AP–sensitive current would not represent activation and inactivation of I_A. Instead, it would depend on the combined effect of both channel blockade and time- and voltage-sensitive unblock. However, we found that at equilibrium high 4-AP concentrations (≥5 mM) completely blocked the early, transient current with no evidence of voltage-dependent unblocking.

To test the results obtained with 4-AP subtraction, we used alternative approaches. Dendrotoxin I (0.5–500 nM), which has been shown to be a specific inhibitor of I_A in

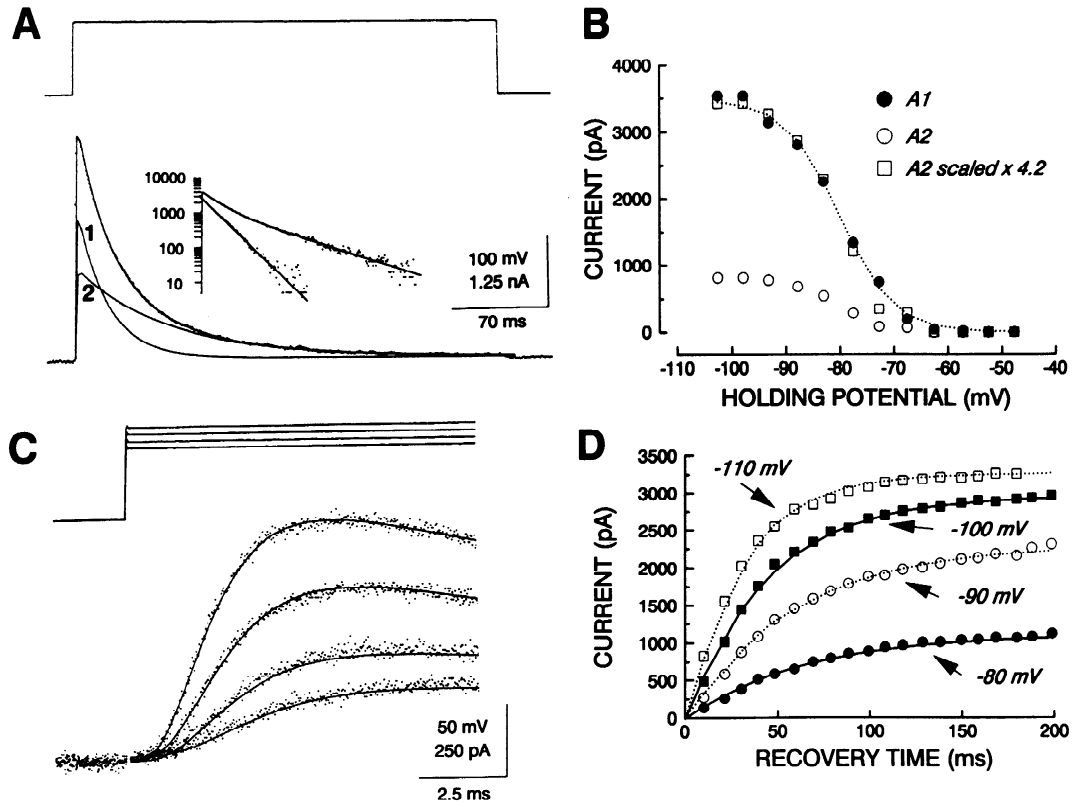

FIG. 6. Voltage-dependent kinetic properties of I_A. *A*: I_A (4-AP–sensitive current) at a command potential of 0 mV from a holding potential of −100 mV. Current rapidly peaks, then completely inactivates. Decay phase was not well fitted by a single exponential. Smooth curve overlapping and indistinguishable from the current trace is the composite of 2 inactivation processes (*traces 1* and *2*). *Inset*: semilog plot of the current with the time-base compressed by a factor of 2. *Top trace* is the composite current and *bottom trace* is the faster, residual current "peeled" from the slower component. Fitting parameters were as follows: amplitude of the fast component (A1) 2,890 pA; slow component (A2) 1,630 pA; fast τ (τ_1) 21.6 ms; slow τ (τ_2) 65 ms. *B*: the 2 decay components of 4-AP–sensitive current display similar steady-state inactivation. Curves at each holding potential were well fitted with 2 components with τs of 21 and 63 ms. Of the 2 components the faster (A1, ●) was larger than the slow (A2, ○); but when scaled (□), the 2 components were well described by the same Boltzman curve. *C*: Rate of activation of I_A at 4 potentials. Curves were fitted with m^4h models with the following values for τ_m: −50 mV, 2.1 ms; −45 mV, 1.7 ms; −40 mV, 1.5 ms; −35 mV, 1.3 ms. *D*: deinactivation of I_A. Holding potential was −20 mV, and hyperpolarizing commands lasting 10–200 ms to potentials between −80 and −110 mV were issued. Fitted curves are shown and values of τ were as follows: −80 mV, 65 ms; −90 mV, 60 ms; −100 mV, 45 ms; −110 mV, 31 ms. Maximum R_s errors: *A*, <1 mV; *B*, <1 mV; *C*, <1 mV; *D*, <2 mV.

other systems (Halliwell et al. 1986), did not block I_A in RNs under these recording conditions. We also designed experiments to isolate I_A by blocking I_T with divalent cations such as Cd^{2+} or Ni^{2+}. This approach was unsuccessful, because even low concentrations (100 μM) of Cd^{2+} caused a large shift in activation (+10 mV) and inactivation (+20 mV) of I_A (cf. Mayer and Sugiyama 1988).

Because 20 mM TEA blocks most of the non-I_A current (e.g., see Fig. 1) and 5 mM 4-AP is a relatively selective blocker of I_A (Fig. 4) with little effect on I_{Ca} ($n = 4$, data not shown), the 4-AP–sensitive current observed in the presence of TEA must be almost entirely due to I_A. An example of 4-AP–sensitive current obtained with a command step to 0 mV is shown in Fig. 6*A*. The fitted curve is the sum of two

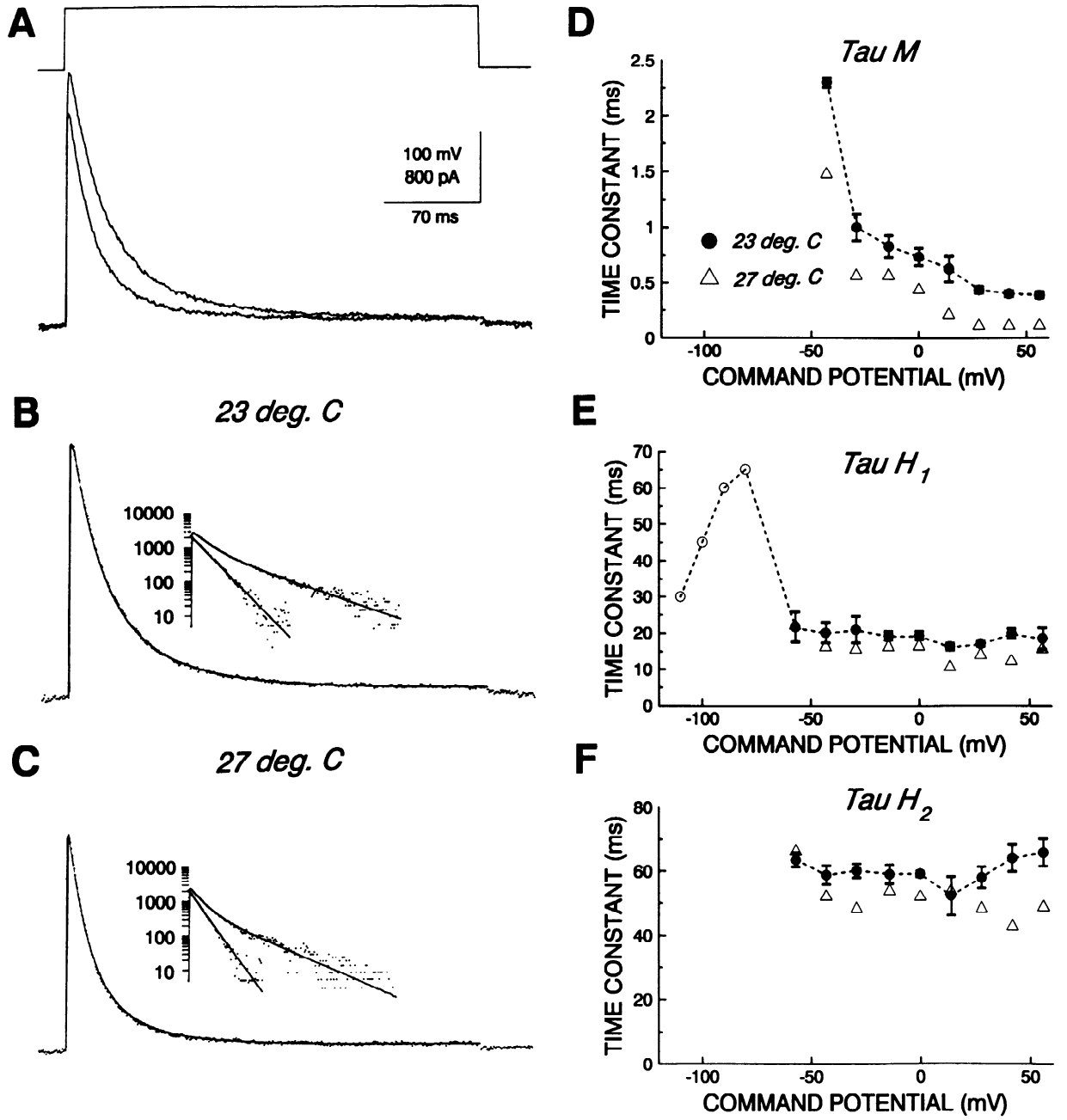

FIG. 7. Voltage and temperature dependence of τ_h and τ_m. *A*: 4-AP–sensitive currents obtained with a command potential of −14 mV at 23°C (larger, slower trace) and 27°C. Peak current amplitudes are similar for these 2 different cells and are overlaid to demonstrate the more rapid kinetics at higher temperatures. *B*: current trace with double exponential fitted curve at 23°C. Semilog *inset* is as in previous figures. Fitting parameters are A_1, 2,270 pA; A_2, 1,060 pA; τ_1, 20.6 ms; τ_2, 60.9 ms; and τ_m, 0.6 ms. *C*: current at 27°C with parameters as follows: A_1, 2,160 pA; A_2, 660 pA; τ_1, 15.5 ms; τ_2, 49.4 ms; and τ_m, 0.4 ms. *D*: voltage dependence of τ_m. 4-AP–sensitive currents were fitted in 4 cells at room temperature (23°C, ●), and 1 cell at 27°C (△). Error bars represent SE. *E*: inactivation of the fast component (τ_1, ●) and recovery from inactivation (○) as a function of voltage and temperature. *F*: voltage dependence of the slow component at room temperature (●) and at 27°C (△). Maximum R_s error, <2 mV.

Hodgkin-Huxley (1952) functions of the form

$$I_A = \left[1 - \exp\left(-\frac{t}{\tau_m}\right)\right]^4 \times \exp\left(-\frac{t}{\tau_h}\right) \times I_\infty \quad (3)$$

where t is time, I_∞ is the current level expected in the absence of inactivation, τ_m is the time constant of activation and τ_h is the time constant of inactivation. For this analysis, it was assumed that the activation time constant (τ_m) was the same for each of the two decay components. The relative amplitudes of the two components were strongly dependent on command potential. With small depolarizations near −40 to −50 mV, the fast component (τ_{h1}) dominated the decay by contributing >90% to the overall process. At 0 mV, τ_{h1} contributed approximately two-thirds; and, at potentials near +20 mV, both components contributed equally. These two components may represent either the composite activity of two types of 4-AP–sensitive channels or the complex inactivation of one population of channels. One piece of evidence to support the latter possibility is the overlap in the steady-state availability functions of the two components (Fig. 6*B*). If the total current were to be accounted for by two populations of channels, these results suggest that each would have to have the same 4-AP dependence and steady-state inactivation properties, which we think unlikely.

With the onset of a depolarizing voltage command, there was a significant delay to the rising phase of the outward current (Fig. 6*C*). This delay was reasonably well fitted by assuming m^4 kinetics. Time-dependent activation of I_A was highly voltage dependent. With increasing depolarizations, both the delay to peak and the corresponding value for τ_m decreased (Figs. 6*C* and 7*D*). Recovery from inactivation (deinactivation) was also voltage dependent (Fig. 6*D*), varying from 65 ms at −80 mV to 31 ms at −110 mV. In contrast to τ_m, inactivation (τ_h) was voltage independent. The fast component, τ_{h1}, was constant at 20 ms for all potentials between −50 and +50 (Fig. 7*E*). Similarly, the slow component, τ_{h2}, was also relatively constant, varying little from a value of 60 ms at any given activation potential (Fig. 7*F*).

Temperature dependence of kinetic rate constants for I_A

Because our experiments were performed at 22–23°C and the temperature coefficient (Q_{10}) of I_A is known to be near 3 in other systems (Connor and Stevens 1971), it is likely that activation and inactivation will be significantly faster at in vivo temperatures. We examined 4-AP–sensitive currents at various temperatures in several cells. Increasing the bath temperature resulted in a marked decrease in τ_m, τ_{h1}, and τ_{h2} so that I_A peak (Fig. 7*A*) occurred with a shorter latency and decayed more rapidly. The two components of decay observed at room temperature were both present at temperatures of 27°C (Fig. 7, *B* and *C*) and above (not shown). Average Q_{10}s for I_A rate constants of both activation and inactivation, determined from seven such experiments performed in the range of 23–35°C, were 2.8 ± 0.3. In four cells the temperature dependence of current amplitude was determined within single cells. Current amplitude also increased with temperature, with a Q_{10} value of 1.6 ± 0.1.

DISCUSSION

RNs of the thalamus possess at least two transient currents, I_A and I_T, which can serve to modulate cellular excitability in the short term (5–50 ms) at membrane potentials near rest. They are both deinactivated by hyperpolarization and activated on release of the hyperpolarizing influence; however, they would tend to have opposite effects on neuronal excitability because their reversal potentials are markedly different, −87 mV for I_A and more than +30 mV for I_T. A more complete understanding of the consequences of the presence of significant amounts of both currents within RNs requires a detailed description of the voltage dependence of activation and inactivation, because small differences in voltage dependence can have significant effects on cell firing behavior. We have presented here a kinetic description of I_A in somatosensory RNs of the rat. I_A was isolated by use of pharmacological tools and voltage protocols, and we recorded the current with low-resistance whole-cell electrodes with series resistance compensation in electrotonically compact cells. The kinetic description of I_A presented here, together with previous similar data on I_T, can be incorporated (along with formal models of other important conductances, including the persistent Na^+ current suggested by current-clamp recordings; Jahnsen & Llinás 1984) into computer simulations that will allow the development of hypotheses regarding the effects of the various near-threshold currents on the firing behavior of RNs. The data on all the relevant conductances are as yet incomplete, but at this point we may speculate as to some of the functions of these two near-threshold currents in thalamic cells.

The activation threshold for I_T is slightly more negative than that for I_A (Fig. 4*D*), and voltage-dependent activation is steeper. Both of these factors will promote the regenerative depolarization that is the LTS. However, the depolarization will eventually begin to activate I_A, which, in turn, will tend to slow the generation of the LTS. The steeper voltage dependence of activation for I_T compared with I_A (Fig. 4) will tend to shift the balance toward depolarization. The time constant of activation is shorter for I_A (Fig. 7*D*) than for I_T (Coulter et al. 1989a). However, because of the m^4 kinetics required for I_A activation compared with m^3 for I_T (Coulter et al. 1989a), the peak current latency for I_A is comparable with that of I_T (cf. Fig. 3,*A* and *B*). We can conclude that some properties of I_T (positive reversal potential; depolarization-promoted increases in both current amplitude and rate of activation) lead to the regenerative activation of a LTS when the opposing current is not sufficient to dampen the depolarization.

An additional consideration is the difference in temperature dependence of the two conductances. Although the rate constants for activation and inactivation of I_A and I_T have similar temperature sensitivities, with Q_{10}s near 3, there are differences in the relationships between current amplitude and temperature. I_T amplitude was found to be highly temperature dependent (Q_{10} = 3.1, Coulter et al. 1989a), in contrast to the lower temperature sensitivity (Q_{10} = 1.6) of I_A amplitude reported here, which is similar to that described for other K^+ and Na^+ currents (Hille 1984). With all other factors being equal, increases in tem-

perature would increase the magnitude of I_T relatively more than that of I_A and thus shift the balance toward depolarization and LTS production.

One of the major kinetic differences between I_A and I_T is the rate of deinactivation. Because I_A recovers from inactivation relatively quickly, there may be significant deinactivation of I_A during a single action potential afterhyperpolarization. I_A may then function in its putative role to set the frequency of slow repetitive firing (Connor and Stevens 1971) during a period when I_T never becomes significantly deinactivated. Thus I_A may serve two roles in regulating RN function, the control of repetitive firing as well as modulation of LTS burst-firing modes.

Modulatory influences on these currents would tend to shift the balance in one direction or another. I_A has been shown to be inhibited by α-adrenergic (Aghajanian 1985) and muscarinic agonists (Akins et al. 1990), whereas I_T is reduced by activators of C-kinase (Marchetti and Brown 1988; Schroeder et al. 1990). These and other factors may influence this system and may thus be important in mediating functional states (such as level of alertness; Steriade and Llinás 1988) or pathophysiological alterations (such as those during generalized epileptiform activity; Coulter et al. 1989b; Gloor and Fariello 1988).

The properties of I_A in relay cells are comparable with those described in other mammalian neurons (Numann et al. 1987; Rogawski 1985; Segal et al. 1984), with a few differences. As in these other examples, inactivation is relatively voltage insensitive; however, in RNs it is made up of two components that make voltage-dependent relative contributions to the composite current. The fast component, with a time constant of 20 ms, is quite similar to that seen in other systems with mild to moderate depolarizations. The slow component, which has not been well documented in other cells, has a time constant of 60 ms and becomes prominent only with depolarizations positive to 0 mV. Both components are blocked by 4-AP; but, as reported in most other systems (Rogawski 1985), concentrations >2 mM are necessary to block the current completely. At these concentrations, the delayed K^+ currents are also significantly affected in relay neurons. Therefore, to isolate I_A, we had to use high concentrations of TEA to block the delayed current before measuring the 4-AP–sensitive current.

In an attempt to compare directly the voltage-dependent gating of I_A and I_T in RNs, we have used pharmacological subtraction. Although this technique is imperfect, it has for the first time allowed this direct comparison to be made in RNs, in which these two currents are especially important in determining cell behavior. The experiments were designed so that 4-AP addition was the only manipulation needed to compare the currents. External divalent ions, which are known to shift voltage-dependent gating for a variety of conductances, were kept constant throughout each experiment. There exists the possibility, however, that the blockers used in this study (4-AP and TEA) may affect the gating of these two currents (and therefore complicate the interpretation of these results), although we found no evidence for such effects. For example, when studied under conditions that isolate I_{Ca}, 4-AP did not affect the gating of I_T. Furthermore, in a variety of tissues, TEA does not affect I_A (Numann et al. 1987; Rogawski 1985). Another concern was that the blocking action may be time dependent. Because the block of I_A by low concentrations of aminopyridines is thought to be voltage dependent (i.e., less effective during depolarization; see Thompson 1982), there may be unblocking during the voltage commands used to elicit the 4-AP–sensitive current (I_A). However, 4-AP at 5 mM was found to block I_A completely, with little evidence of voltage-dependent unblocking, so this would not be a significant source of error when the current subtraction technique was employed. Furthermore, there is little evidence for voltage-dependent block by external TEA (Armstrong and Hille 1972). Finally, the qualitative findings of this study do not depend entirely on pharmacological subtraction. Nonexponential decay, voltage-dependent rate of activation, and voltage-independent rate of inactivation were all evident in the raw current traces recorded in the presence of TEA alone. These currents are largely composed of I_A, because the currents remaining after the addition of 4-AP were relatively small (<10% of maximum I_A).

A variety of rat brain K^+ channel subunits have been cloned and studied in amphibian expression systems (Stühmer et al. 1989). It is interesting to note that none of these has properties entirely consistent with those of the I_A seen in RNs. A candidate that expresses some similarities is RCK4, which is inactivating (albeit more slowly than RN I_A, with $\tau_h \approx 100$ ms) and insensitive to TEA; however, it is relatively insensitive to 4-AP. Such differences might occur if there is altered expression in the *Xenopus* oocytes or if I_A is not a homomultimer of RCK4 subunits but rather is a heteromultimer of RCK4 and other subunit types (e.g., Ruppersberg et al. 1990).

We thank E. Brooks and I. Parada for technical assistance.

This work was supported by National Institute of Neurological Disorders and Stroke Grants NS-06477, NS-12151, and NS-07280 and the Morris and Pimley Research Funds.

Present address of D. A. Coulter: Dept. of Neurology, PO Box 599, MCV Station, Richmond, VA 23298.

Received 4 February 1991; accepted in final form 31 May 1991.

REFERENCES

AGHAJANIAN, G. K. Modulation of a transient outward current in serotonergic neurones by alpha 1-adrenoceptors. *Nature Lond.* 315: 501–503, 1985.

AKINS, P. T., SURMEIER, D. J., AND KITAI, S. T. Muscarinic modulation of a transient K^+ conductance in rat neostriatal neurons. *Nature Lond.* 344: 240–242, 1990.

ARMSTRONG, C. M. AND HILLE, B. The inner quaternary ammonium ion receptor in potassium channels of the node of Ranvier. *J. Gen. Physiol.* 59: 388–400, 1972.

BEZANILLA, F. AND ARMSTRONG, C. M. Inactivation of the sodium channel. I. Sodium current experiments. *J. Gen. Physiol.* 70: 549–566, 1977.

CACECI, M. S. AND CACHERIS, W. P. Fitting curves to data. *Byte* May: 340–362, 1984.

CONNOR, J. A. AND STEVENS, C. F. Voltage clamp studies of a transient outward membrane current in gastropod neural somata. *J. Physiol. Lond.* 213: 21–30, 1971.

COULTER, D. A., HUGUENARD, J. R., AND PRINCE, D. A. Calcium currents in rat thalamocortical relay neurones: kinetic properties of the transient, low-threshold current. *J. Physiol. Lond.* 414: 587–604, 1989a.

COULTER, D. A., HUGUENARD, J. R., AND PRINCE, D. A. Specific petit mal anticonvulsants reduce calcium currents in thalamic neurons. *Neurosci. Lett.* 98: 74–78, 1989b.

COULTER, D. A., HUGUENARD, J. R., AND PRINCE, D. A. Differential

effects of petit mal anticonvulsants and convulsants on thalamic neurones: calcium current reduction. *Br. J. Pharmacol.* 100: 800–806, 1990.

CRUNELLI, V., LIGHTOWLER, S., AND POLLARD, C. A T type calcium current underlies the low threshold calcium potential in cells of the cat and rat lateral geniculate nucleus. *J. Physiol. Lond.* 413: 543–561, 1989.

DESCHÊNES, M., ROY, J. P., AND STERIADE, M. Thalamic bursting mechanism: an inward slow current revealed by membrane hyperpolarization. *Brain Res.* 239: 289–293, 1982.

FORSCHER, P. AND OXFORD, G. S. Modulation of calcium channels by norepinephrine in internally dialyzed avian sensory neurons. *J. Gen. Physiol.* 85: 743–763, 1985.

FRANKENHAEUSER, B. AND HODGKIN, A. L. The after-effects of impulses in the giant nerve fibres of *Loligo*. *J. Physiol. Lond.* 131: 341–376, 1956.

GLOOR, P. AND FARIELLO, R. G. Generalized epilepsy: some of its cellular mechanisms differ from those of focal epilepsy. *Trends Neurosci.* 11: 63–68, 1988.

HALLIWELL, J. V., OTHMAN, I. B., PELCHEN-MATTHEWS, A., AND DOLLY, J. O. Central action of dendrotoxin: selective reduction of a transient K conductance in hippocampus and binding to localized acceptors. *Proc. Natl. Acad. Sci. USA* 83: 493–497, 1986.

HAMILL, O. P., MARTY, A., NEHER, E., SAKMANN, B., AND SIGWORTH, F. J. Improved patch-clamp techniques for high-resolution current recording from cells and cell-free membrane patches. *Pfluegers Arch.* 391: 85–100, 1981.

HERNÁNDEZ-CRUZ, A. AND PAPE, H.-C. Identification of two calcium currents in acutely dissociated neurons from the rat lateral geniculate nucleus. *J. Neurophysiol.* 61: 1270–1283, 1989.

HILLE, B. *Ionic Channels of Excitable Membranes.* Sunderland, MA: Sinauer, 1984.

HODGKIN, A. L. AND HUXLEY, A. F. A quantitative description of membrane current and its application to conduction and excitation in nerve. *J. Physiol. Lond.* 117: 500–544, 1952.

HUGUENARD, J. R., COULTER, D. A., AND PRINCE, D. A. Whole-cell clamp of rat thalamic neurons reveal two distinct transient K currents. *Soc. Neurosci. Abstr.* 16: 507, 1990.

HUGUENARD, J. R. AND PRINCE, D. A. Slow inactivation of a TEA-sensitive K current in acutely isolated rat thalamic relay neurons. *J. Neurophysiol.* 66: 1316–1328, 1991.

JAHNSEN, H. AND LLINÁS, R. Ionic basis for the electroresponsiveness and oscillatory properties of guinea-pig thalamic neurones in vitro. *J. Physiol. Lond.* 349: 227–247, 1984.

KAY, A. R. AND WONG, R. K. S. Isolation of neurons suitable for patch-clamping from adult mammalian central nervous systems. *J. Neurosci. Methods* 16: 227–238, 1986.

MARCHETTI, C. AND BROWN, A. M. Protein kinase activator 1-oleoyl-2-acetyl-*sn*-glycerol inhibits two types of calcium currents in GH3 cells. *Am. J. Physiol.* 254 (*Cell Physiol.* 23): C206–C210, 1988.

MAYER, M. L. AND SUGIYAMA, K. A modulatory action of divalent cations on transient outward current in cultured rat sensory neurones. *J. Physiol. Lond.* 396: 417–433, 1988.

NUMANN, R. E., WADMAN, W. J., AND WONG, R. K. S. Outward currents of single hippocampal cells obtained from the adult guinea-pig. *J. Physiol. Lond.* 393: 331–353, 1987.

ROGAWSKI, M. A. The A-current: how ubiquitous a feature of excitable cells is it? *Trends Neurosci.* 8: 214–219, 1985.

RUPPERSBERG, J. P., SCHRÖTER, K. H., SAKMANN, B., STOCKER, M., SEWING, S., AND PONGS, O. Heteromultimeric channels formed by rat brain potassium-channel proteins. *Nature Lond.* 345: 535–537, 1990.

SCHROEDER, J. E., FISCHBACH, P. S., AND MCCLESKEY, E. W. T-type calcium channels: heterogeneous expression in rat sensory neurons and selective modulation by phorbol esters. *J. Neurosci.* 10: 947–951, 1990.

SEGAL, M., ROGAWSKI, M. A., AND BARKER, J. L. A transient potassium conductance regulates the excitability of cultured hippocampal and spinal neurons. *J. Neurosci.* 4: 604–609, 1984.

STERIADE, M. AND LLINÁS, R. R. The functional states of the thalamus and the associated neuronal interplay. *Physiol. Rev.* 68: 649–742, 1988.

STÜHMER, W., RUPPERSBERG, J. P., SCHRÖTER, K. H., SAKMANN, B., STOCKER, M., GIESE, K. P., PERSCHKE, A., BAUMANN, A., AND PONGS, O. Molecular basis of functional diversity of voltage-gated potassium channels in mammalian brain. *EMBO J.* 8: 3235–3244, 1989.

SUZUKI, S. AND ROGAWSKI, M. A. T-type calcium channels mediate the transition between tonic and phasic firing in thalamic neurons. *Proc. Natl. Acad. Sci. USA* 86: 7228–7232, 1989.

THOMPSON, S. H. Three pharmacologically distinct potassium channels in molluscan neurones. *J. Physiol. Lond.* 265: 465–488, 1977.

THOMPSON, S. H. Aminopyridine block of transient potassium current. *J. Gen. Physiol.* 80: 1–18, 1982.

YELLEN, G. Single Ca^{2+}-activated non-selective cation channels in neuroblastoma cells. *Nature Lond.* 296: 357–359, 1982.